Charge Transport Across Insulating Self-Assembled Monolayers: Non-equilibrium Approaches and Modeling To Relate Current and Molecular Structure

Fatemeh Mirjani,*,† Joseph M. Thijssen,‡ George M. Whitesides,¶,⊥ and Mark A. Ratner§

†Chemical Engineering Department, Delft University of Technology, Julianalaan 136, 2628 BL Delft, The Netherlands, ‡Kavli Institute of Nanoscience, Delft University of Technology, Lorentzweg 1, 2628 CJ Delft, The Netherlands, ¶Department of Chemistry and Chemical Biology, Harvard University, 12 Oxford, Cambridge, Massachusetts 02138, United States, ⊥Kavli Institute for Bionano Science and Technology, Harvard University, 29 Oxford, Cambridge, Massachusetts 02138, United States, and §Department of Chemistry and Non-Equilibrium Research Center, Northwestern University, 2145 Sheridan Road, Evanston, Illinois 60208-3113, United States

ABSTRACT This paper examines charge transport by tunneling across a series of electrically insulating molecules with the structure $HS(CH_2)_4CONH(CH_2)_2R$) in the form of self-assembled monolayers (SAMs), supported on silver. The molecules examined were studied experimentally by Yoon *et al.* (*Angew. Chem. Int. Ed.* 2012, *51*, 4658−4661), using junctions of the structure $AgS(CH_2)_4CONH(CH_2)_2R//Ga_2O_3$/EGaIn. The tail group R had approximately the same length for all molecules, but a range of different structures. Changing the R entity over the range of different structures (aliphatic to aromatic) does not influence the conductance significantly. To rationalize this surprising result, we investigate transport through these SAMs theoretically, using both full quantum methods and a generic, independent-electron tight-binding toy model. We find that the highest occupied molecular orbital, which is largely responsible for the transport in these molecules, is always strongly localized on the thiol group. The relative insensitivity of the current density to the structure of the R group is due to a combination of the couplings between the carbon chains and the transmission inside the tail. Changing from saturated to conjugated tail groups increases the latter but decreases the former. This work indicates that significant control over SAMs largely composed of nominally insulating groups may be possible when tail groups are used that are significantly larger than those used in the experiments of Yoon *et al.*[1]

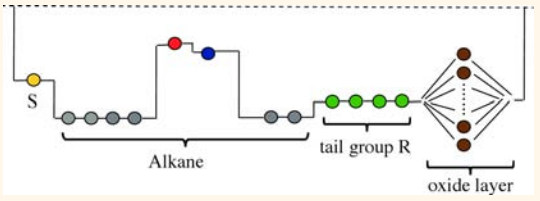

KEYWORDS: molecular electronics · self-assembled monolayers · molecular structure · charge transport · hole tunneling · current density

The putative field of "Molecular Electronics" involves charge transport by processes in which the structure of the molecule forming the junction influences the conductance. The ultimate aim is to design molecules whose electrical conductance can be tuned rationally through organic synthesis.[2−8] One of the motivations for this field has been the expectation that small changes in the structure or the environment of the molecules would change the characteristics of charge transport through them in ways that might be useful in practical electronics, sensing, or controls. In single molecule devices with weak electrode/molecule interaction, Coulomb blockade enables switching the current on and off by a gate field.[9,10] This type of control is, however, not the only way to control the current. Fracasso *et al.*[11] showed that the conductance in anthracene derivatives of approximately the same thickness can be influenced by the type of conjugation. The results in that experiment[11] were attributed to quantum interference, but the origin of the effect remains to be validated in other experiments. There are now many reports of substantially different conductance values measured in break junctions (see *e.g.*, ref 12). Another example is the exponential decay of the conductance in alkane self-assembled monolayers (SAMs),

* Address correspondence to fateme.mirjani@gmail.com.

Received for review September 10, 2014 and accepted November 14, 2014.

Published online November 14, 2014
10.1021/nn505115a

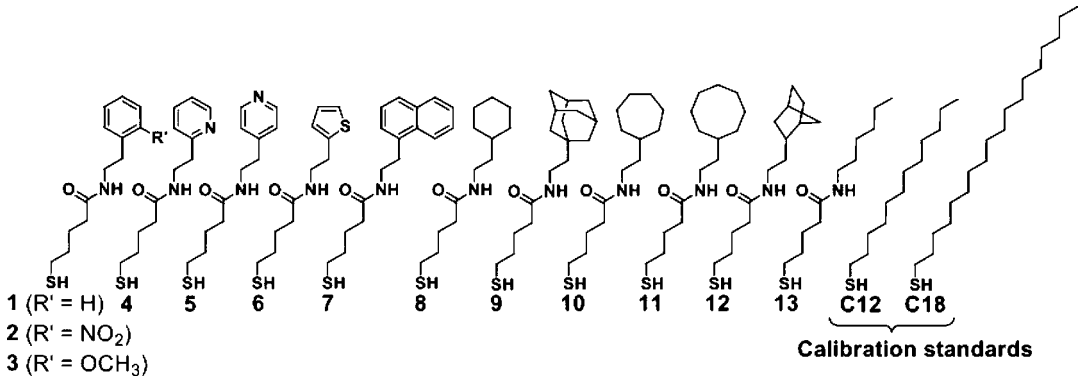

Figure 1. Structure of the molecules used by Yoon *et al.*[1] to form the self-assembled monolayers on the Ag surface. The structure of all molecules 1−13 is $HS(CH_2)_4CONH(CH_2)_2-R$ where R is the tail group. In the measurements, molecules C12 and C18 were presented as calibration standards. All current densities were measured through Ag-molecule-Ga_2O_3/EGaIn structures.

which does not exist in *n*-polyene chains in which a chain of C−C single bonds $(CH_2)_{2n}$ is replaced by an extended conjugated chain $(CH{=}CH_2-)_n$.[13]

Yoon *et al.*,[1] reported a systematic experimental study in SAMs which suggested that large changes in molecular structure (*e.g.*, changing a cyclohexyl group for a phenyl group) need not induce significant changes in the conductance of molecular monolayers. Yoon's study also indicated that replacing[1] $-CH_2CH_2-$ in the interior of the molecules making up the SAMs by −CONH− had no effect on tunneling current. More specifically, they measured the current densities through a series of SAMs based on different molecules located between a silver electrode and Ga_2O_3/EGaIn electrode, where EGaIn denotes eutectic gallium and indium (a liquid metal alloy[14]) and Ga_2O_3 is a spontaneously formed, electrically conducting surface oxide layer (normally 0.7 nm thick) on the EGaIn electrode. The structure of the molecules making up the SAMs is $HS(CH_2)_4CONH(CH_2)_2R$ where R is one of the tail groups shown in Figure 1. In all these molecules, the tail groups have almost the same length. The tail structures can be divided into two groups: (1) aromatic structures and (2) saturated aliphatic groups.

It is not obvious why SAMs of these very different molecules do not yield very different conductivities. (Examination of the values of the current density in Figure 2 suggests that aromatic tail groups might be slightly (2 times) more conducting than aliphatic ones; we have however taken the conservative point of view based on the statistically well-defined standard deviation that statistically we cannot distinguish aliphatic and aromatic tail groups.) The measured current densities for all molecules at V_{bias} = 0.5 V are shown in Figure 2 on a logarithmic scale, with simple alkane chains of length 12 and 18 alkane units (e.g., $S(CH_2)_{n-1}CH_3$) included. Alkane chains are standard molecules in which electron transport has been studied extensively.[15−22] The main result of those prior studies is that the current decays exponentially with chain length with a decay constant $\beta \sim 1.0$

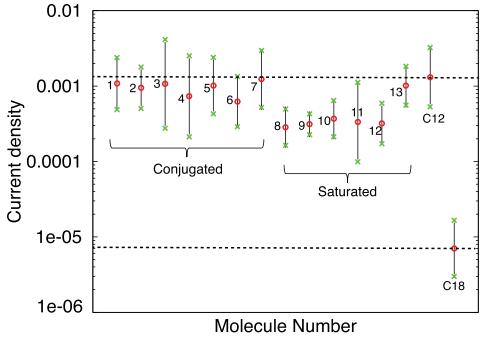

Figure 2. Current density measured by Yoon *et al.*[1] at V_{bias} = 0.5 *V* for the molecules of Figure 1 (presented on a logarithmic scale). The unit of the current density is A/cm^2. The green crosses (×) show the interval of the errors. Although the saturated structures (molecules 8−13) seem to have a somewhat smaller conductance than the conjugated ones (molecules 1−7), the differences are not significant within the experimental error.

per CH_2 unit, with some variation across different experiments.[15−19,23] This dependence has been also successfully addressed computationally using Density Functional Theory (DFT) combined with the non-equilibrium Green's function (NEGF) studies.[16,22,24] Yoon *et al.* measured $\beta \sim 0.9$ per CH_2 unit, a value that is in agreement with these earlier results. In fact, the 12- and 18-unit alkane chains are used as calibration standards in Yoon's experiment, to compare with the results obtained with the other molecules.

Understanding the relatively constant current density observed for this complicated system is difficult, as different mechanisms may be responsible for the observed current densities. While interchain tunneling of the electrons may be significant, here we focus on the effects of the molecular electronic structure on the single-molecule current. The standard way to address this subject is by performing DFT−NEGF calculations.[25,26] We did such calculations, which confirm that varying the tail group does not induce dramatic differences in the molecular conductance. To understand this result, we describe the transport using a simple tight-binding model, with parameters inferred

from a series of ground-state DFT calculations. We call this the *tight-binding toy model* (TBTM). The procedure we follow is in the spirit of semiempirical models which aim to explain experiments using parameters obtained *via* fitting to *ab initio* calculations or to experimental data. In particular, one of the criteria we have used to adjust the parameters is that the structure of a few of the highest occupied frontier orbitals, as obtained by full DFT calculations, is essentially reproduced in TBTM. The transmission of the model is then analyzed again using Green's function methods. This provides insight into why the current varies only weakly across the set. These results may help designing future experiments to synthesize molecules with substantially different transmissions.

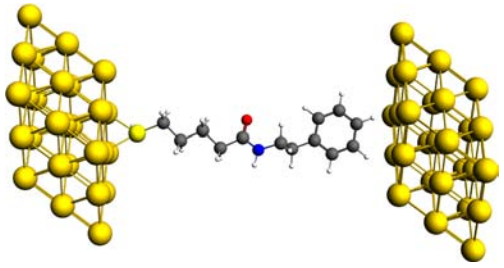

Figure 3. Structure of the *extended molecule* 1 in which the molecule is connected to 3 × 3 × 3 Au clusters from left and right.

DFT Calculations. *DFT−NEGF-Based Transport Calculations.* We start with the transmission for molecules 1−13 obtained from DFT−NEGF. We have calculated the transmission through these molecules with two different methods (see Methods section for details):

(I) Gas-phase NEGF. In this method, DFT calculations for molecules in the gas phase (thiol-ended, without electrodes) are performed, and then the contribution of the molecule to transport is calculated, using the converged Hamiltonian for the molecule. (II) Extended molecule-NEGF: In this method, an *extended molecule* is used. The extended molecule is made by connecting the molecule to gold clusters from right and left, see Figure 3.

The transmission results for both methods are shown in Figure 4. In all molecules 1−13, the transmission peaks below the Fermi energy are closer to the Fermi energy than the peaks above the Fermi energy, indicating that the transport is hole-like. The influence of the metal in the calculation is reflected in the shift and broadening of transmission peaks. By integrating the transmission curves obtained using the gas-phase molecules over the voltage range between −0.25 and

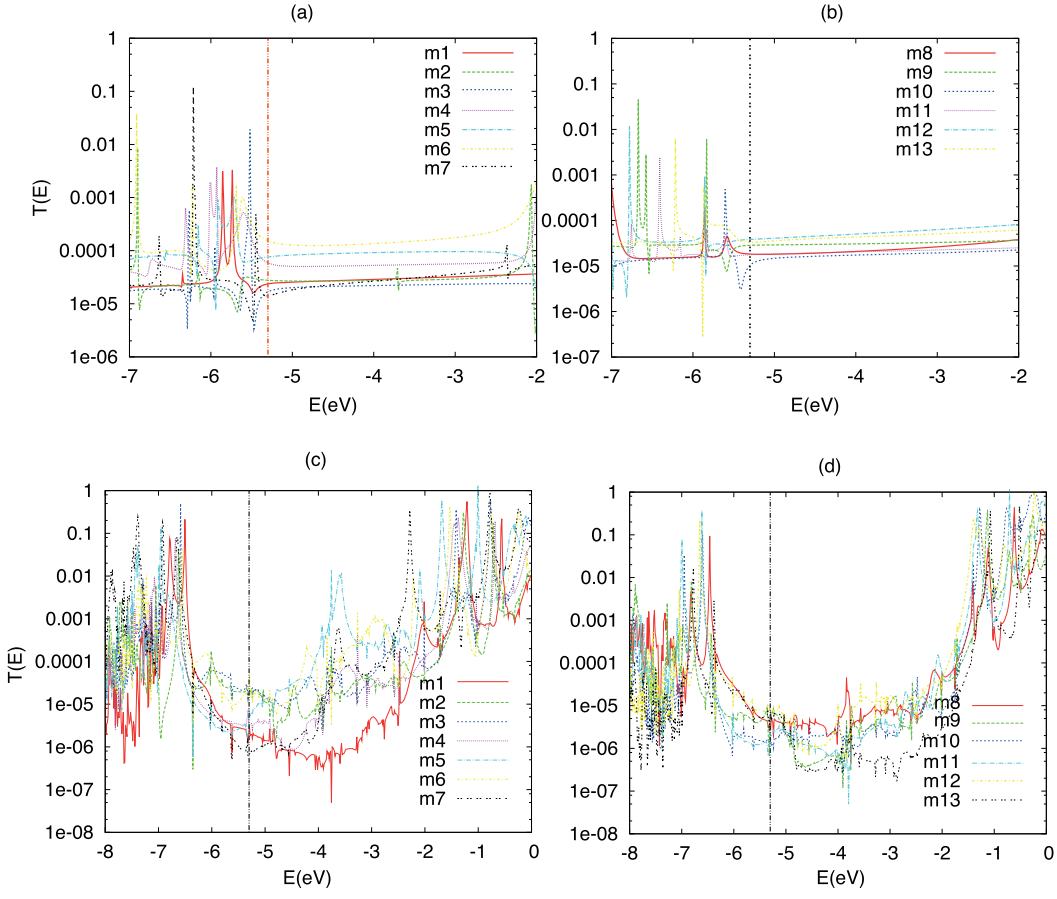

Figure 4. Transmission through molecules 1−7 (with conjugated tail groups) and molecules 8−13 (with saturated tail groups) on a logarithmic scale. The vertical dashed lines show the Fermi energy at −5.3 eV: (a,b) gas phase-NEGF; (c,d) extended molecule-NEGF in which the extended molecules consist of molecules and two 3 × 3 × 3 Au clusters.

0.25 V (corresponding to symmetric bias drop and a temperature of 0 K), we obtain the currents shown in Figure 5 which do not differ by more than a factor of 8 (results for the extended molecule are presented in the Supporting Information). The fact that conjugated groups give slightly larger currents than the saturated ones in the experiment is not reproduced, probably due to the coupling to the oxide layer which is not included in this calculation. The extended molecule results are in better agreement on this point (see Supporting Information). In the next sections, we will develop a toy model which explains why the current through these structures shows only a modest variation.

Molecular Orbitals. We have performed ground state DFT calculations for the molecules in the gas phase (see Methods section for details). The results give insight into the behavior of the electrons participating in transport, and help us to construct the TBTM Hamiltonian describing the landscape in which the electrons are moving. The highest occupied molecular orbital (HOMO) and lowest unoccupied molecular orbital (LUMO) are shown in Figure 6.

From these results, we observe the following:

(I) The HOMO orbital for all molecules is localized on the sulfur atom bonded to the Ag surface in the experiment. Both the HOMO energy and its shape are approximately the same for all molecules.

(II) The LUMO structure and energy vary quite strongly with tail group. The shape of the LUMO furthermore depends quite sensitively on the geometrical optimization. With our optimized geometries (that may or may not agree in detail with the structures found in the SAMs, which are not known in detail experimentally, and probably depend on the topography of the electrode surface), the LUMO of the molecules with saturated tail groups is located on the thiol group just as the HOMO, whereas for molecules with a conjugated tail group, it is located on the tail group.

(III) HOMO-1, HOMO-2, and HOMO-3 of molecules 1−13 are mostly located on the amide, on both the amide and the tail group R, and on the tail group R, respectively (see Supporting Information).

As the structure and chemical potential of the HOMO does not change substantially across different molecules, and as the HOMO is substantially closer to the Fermi energy of the electrodes (E_F(Ag) = −4.7 eV, E_F(Ga_2O_3/EGaIn) = −4.3 eV[1]) than the LUMO, we expect the transport to be hole-like, that is, dominated

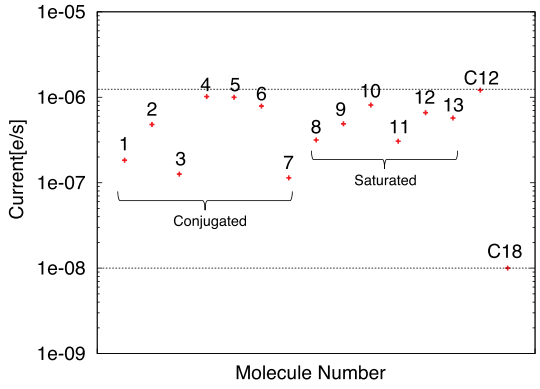

Figure 5. Current (shown on a logarithmic scale) obtained from gas phase-NEGF method, by integrating the transmission from −0.25 to 0.25 V. These results clearly show that the variations in transmission through these different molecules are modest, in agreement with the results for the current obtained by Yoon *et al.*[1]

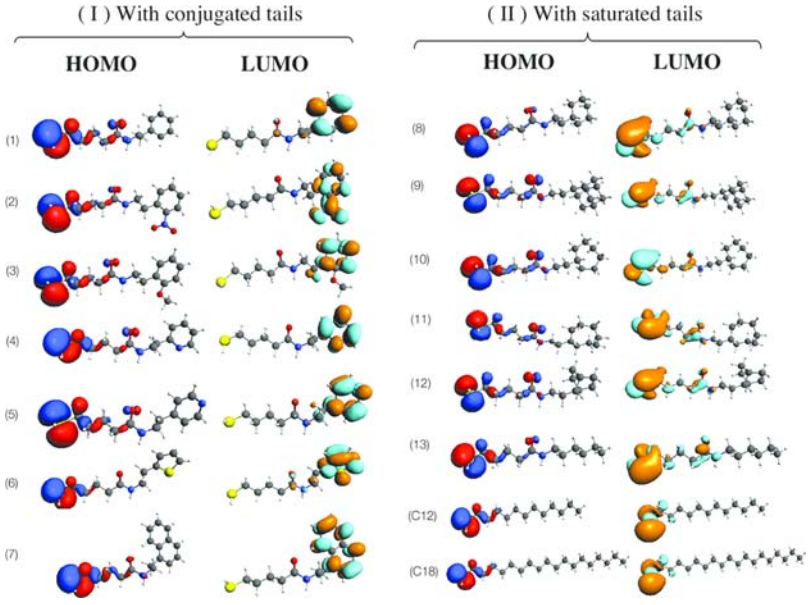

Figure 6. HOMO and LUMO of the molecules 1−13 from the DFT calculation. Molecules C12 and C18 were presented in the experiment as calibration standards. The HOMO of all of these molecules is largely localized on the thiol linker. The LUMO is localized on the tail group in molecules 1−7, which have conjugated tails. However, in molecules 8−13 with saturated tails, the LUMO is mostly localized on the thiol group.

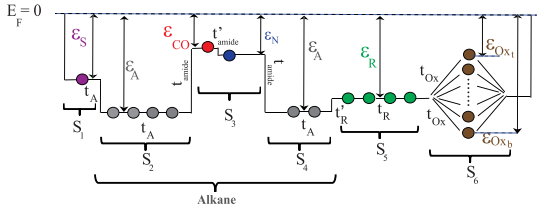

Figure 7. A tight-binding toy model (TBTM) structure representing the molecules 1−13 and the oxide layer. We model the molecular junction with six segments S_1−S_6. The barriers with different site energies represent the following parts of the molecules: ε_S, thiol group; ε_A, alkane chain in which the energy of the central sites (ε_{CO} and ε_N) are chosen to be higher than the rest of subunits; they represent the amide group (CONH); ε_R, tail group R (which varies in molecules 1−15); ε_{Ox}, Ga_2O_3 layer.

through the HOMO, in agreement with our NEGF calculations.

Tight-Binding Model. The DFT-based NEGF calculations just presented do reproduce the experimentally observed insensitivity of the current to the chemical composition of the tail group. To obtain a better understanding of this result, and to analyze the junction with a nonmetallic electrode, we construct a simple tight-binding toy model (TBTM). The model Hamiltonian is designed such that the electrons and their dynamics reflect the behavior of electrons described by a full DFT Kohn−Sham Hamiltonian, as used in the previous section. This implies that the TBTM parameters, especially those which influence the energetics of low-lying occupied states, do not necessarily reflect spectral features (which are known to be badly reproduced by DFT). The guiding principle in constructing the TBTM model is that it produces reliable HOMOs, as the transport in the molecules under study is hole-like and off-resonant (see previous section).

We want the tight-binding chain in our toy model to mimic the electronic properties of molecules 1−15. These molecules consist of six segments (Figure 7) The first segment (S1) is the thiol linker and the next three segments are S2 $(CH_2)_4$, S3 CONH, and S4 $(CH_2)_2$, respectively. The next part (S5) is the tail group R and the last segment (S6) is the oxide layer. We find most of the parameters of the TBTM Hamiltonian of eq 1 from the frontier orbitals shown in Figure 6 and in the Supporting Information, and from calculations on periodic chains, as we outline in the Supporting Information. In the Supporting Information, details about the procedure for finding the parameters and validations of the results can be found.

Our generic tight-binding chain for molecules 1−13 is shown in Figure 7. It consists of 17 sites, divided into six subunits. The first molecular subunit (S_1) represents the thiol binding group connected to the silver electrode. Its site energy, ε_S, is higher than that of the alkane chain. The following three *groups* of sites (S_2, S_3, S_4) represent the alkane chain with the amide. The amide sites (S_3) have energies ε_{CO} and ε_N that are higher than those of alkanes. It should be noted that our model presents a coarse-grained description of the molecules under study. In particular, in our description of the amide units, the (C═O) group is considered as one site, and the (NH_2) as another one.

TABLE 1. Tight-Binding Parameters ε and t for Each Subunit (in eV)[a]

subunit	site number	represent	ε	t, t_n	ε (lit.)	t (lit.)
S_1	1	thiol	−4.2	6, 6		
S_2	2−5	methylenes	−14	6	−13.9[a]	6[b], 7.7[c]
S_3	6−7	amide	−1.3, −1.8	0.5, 1.8		1.8[d]
S_4	8−9	methylene	−14	6	−13.9[a]	6[b], 7.7[c]
S_5	10−13	saturated tail group R	−14	6	−13.9[a]	6[b], 7.7[c]
S_5	10−13	conjugated tail group R	3.5	4, 1	5.9[e]	4[e], 3.6[a]
S_6	14−N	Ga_2O_3	−4.5 to −11.5			

[a] Subunits of the same kind are coupled by t. The coupling of a subunit to a saturated C neighbour is t_n, provided the subunit itself is not a saturated C (including methylene). Literature parameters are presented from (a) Benkö *et al.*,[31] (b) Xu *et al.*,[32] (c) Wang *et al.*,[33] (d) Murrell,[34] and (e) Salem.[35] t parameter for the last subunit is zero as it includes a series of uncoupled sites which mimic the band structure of the oxide layer. All sites in this subunit are coupled to the last site of the tail group by $t = 0.1$. For details, see Supporting Information.

Two amide subunits (C═O and NH) are coupled to neighboring CH_2 by t_{amide}^{-}; we take those to be the same. The coupling inside the amide group is $t_{amide}^{'}$. The fourth substructure S_4, represents the two methylene sites between amide and R. The tail group R (which varies in molecules 1−13) is denoted as S_5 and couples to the alkane part with $t_R^{'}$. As the size of R is approximately the same in molecules 1−13, we fix the length of S_5 to four sites. The last subunit, S_6, represents the Ga_2O_3 layer. This subunit includes a series of uncoupled sites which mimic the band structure of the oxide layer. The top site with energy level ε_{Ox_t} represents the top of the band of this layer, and similarly the parameter ε_{Ox_b} corresponds to the bottom of the band. All the sites in this subunit are coupled to the last site of the tail group by t_{Ox}. The only parameters that change across molecules 1−13 are the site energy and the tunneling parameters describing S_5, that is, ε_R, t_R, and $t_R^{'}$, where $t_R^{'}$ describes the coupling to the CH_2 group.

The orbitals found in DFT are evaluated with a potential corresponding to the neutral molecule. Our method is in the spirit of semiempirical models like extended Hückel,[27] PPP,[28] CNDO,[29] MNDO,[30] *etc.*, which fit the tight-binding parameters to *ab initio* calculations or to experimental data.

The tight-binding parameters ε and t for each subunit are shown in Table. 1. In Hückel molecular orbital theory, these parameters are called α and β, respectively. The agreement between our TB parameters and similar parameters obtained by others (see the values in the last four columns of Table 1, together with the fact

that they can be varied over a finite range without affecting the results, suggests that most of them are transferable. Exceptions are the amide parameters, which require careful tuning. We therefore expect these to be rather specific for the arrangement of this group in the molecules studied here.

RESULTS FOR THE CURRENT

Once the molecule is coupled to the electrodes, the retarded Green's function of the system can be obtained as $G^R = [\omega S - H - \Sigma]^{-1}$, where Σ is the total self-energy obtained from left (L) and right (R) self-energies, $\Sigma = \Sigma^L + \Sigma^R$. Within the wide band limit (WBL), Σ^L and Σ^R are purely imaginary and do not depend on energy. They represent the broadenings $\Sigma^{L/R} = (-i/2)\Gamma^{L/R}$. Once the Green's functions are known, the current can be calculated from a Landauer-type equation:

$$I = \frac{ie}{h}\int \mathrm{d}\,\omega T(\omega)\,[f(\omega,\mu_L) - f(\omega,\mu_R)] \qquad (1)$$

where

$$T(\omega) = \mathrm{Tr}\{\Gamma_L G^r \Gamma_R G^a\} \qquad (2)$$

is the transmission, $\mu_L = E_f - V/2$, $\mu_R = E_f + V/2$ and G^a is the advanced Green's function which is found as the complex conjugate of G^r. The Fermi function $f(\omega,\mu)$ describes the electronic occupation of the levels, $f(\omega,\mu) = 1/(1 + \exp((\omega - \mu)/(kT)))$. The Γ parameters describe the molecule−electrode coupling and are assumed the same for all molecules in our calculation.

The only parameters that change across molecules 1−13 are the site energy and the tunneling parameters of S_5, that is, ε_R, t_R, and t'_R, representing the tail group. To study the transport through molecules 1−13, we calculate the current for different values of these three parameters. It should be noted that in matching the orbital structure from our TBTM to the DFT results, we have found it sometimes necessary to shift the site energies of the tail group somewhat (see Supporting Information). The variation of ε_R evaluated from DFT is ∼1 eV. Our results for molecules with conjugated and saturated tails and in the presence of a bias voltage are shown in Figure 8. They show that the largest difference in the current is a factor of ∼7.6 at a bias voltage V_b = 0.5 eV. This result agrees well with the results of the experiment (measured at bias 0.5 eV). In addition, the allowed amount of variation for these parameters to reproduce the main features of the orbital structure and current is ±0.3 eV.

The structures of some tail groups in Figure 1 are not linear. Therefore, we also investigate the transport through a system with a cyclic tail group as shown in Figure 9, which provides two pathways for the particles moving through the tight-binding chain. The current through such a chain is compared to the results of the original model of Figure 7 both for molecules with conjugated (ε_R = 3.5, t_R = 4, t'_R = 1) and saturated (ε_R = −14, t_R = 6, t'_R = 6) tail groups. We emphasize that, although the difference between the site energies for pi- and sigma-orbitals seems rather dramatic (3.5 *versus* −14 eV), this does not imply a similar difference in chemical potential: as the pi-system is only half filled in the neutral state, the highest occupied pi-level is still below the ϵ for pi-sites, and for the R-groups we consider here they turn out to be about 1 eV below the Fermi energy of the gold. The sigma orbitals are all filled and therefore reach up to $\epsilon + 2\tau \approx -14 + 2\cdot 6 = -2$ eV. As shown in Figure 9, the current

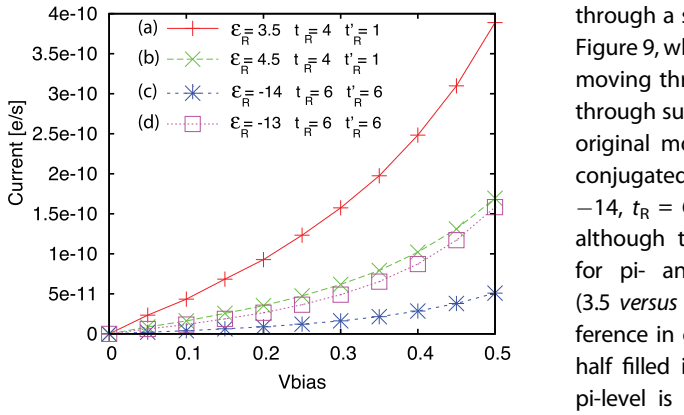

Figure 8. Current for different parameter values. For the cases (a), (b), (c) and (d), the frontier orbitals are shown the Supporting Information. The ratio of the current variation with respect to current in case (a) at voltage V_b = 0.5 eV changes at most by a factor of ∼7.6.

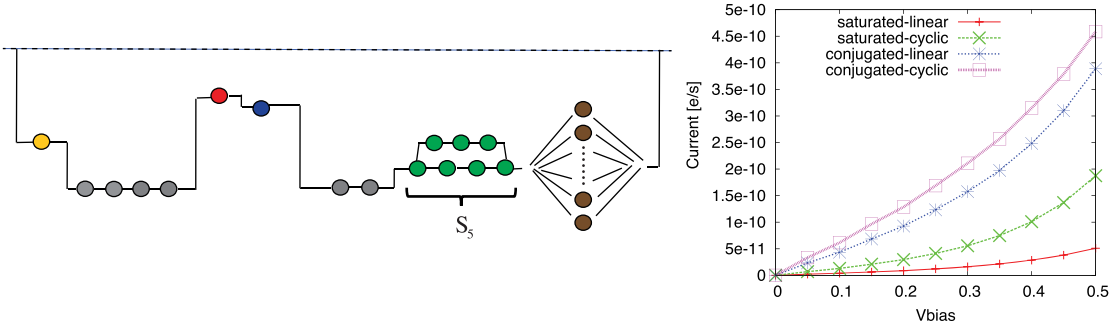

Figure 9. Current for the molecules shown in Figure 8, but with the linear segment S_5 representing the tail group R, replaced by a cyclic chain which provides two pathways for the electrons going through the tight-binding chain. For conjugated groups, ε_R = 3.5, t_R = 4, t'_R = 1. For saturated groups, ε_R = −14, t_R = 6, t'_R = 6.

through the molecules with cyclic structure is in the same range of molecules with linear tails, and the largest overall change between the $I-V$ curves is a factor of 8.

As shown in the Supporting Information, the variation of ε_R evaluated from DFT is not large (~1 eV). Within this variation the highest occupied orbitals, which are largely responsible for the transport, are always localized on specific regions of the molecules. For instance, the HOMOs in all molecules are located on the thiol anchoring group. However, the shape of the tunneling barrier is determined by the entire tunneling chain which contains the tail group at the end of the chain. Therefore, the transmission through the tail group is important. Our analysis indicates that the combination of t_R and t_R' compensates for the variation of the site energy, ε_R, which is close to the Fermi energy in conjugated groups, whereas in saturated groups it is far from the Fermi energy (remember that the TBTM model was not designed to yield excitation energies; see the Tight-Binding Model section). In other words, the gateway from a saturated orbital to a conjugated electron system on the tail group can be viewed as a narrow passage leading to an easily traversable track. Moving from the conjugated chain to a saturated tail group is easy (the t-matrix element is large), but the orbital energy is much farther away from the Fermi energy, suppressing the current through this structure.

CONCLUSIONS

We have investigated the transport through a series of self-assembled monolayers with varied tail groups, as measured by Yoon *et al.*[1] DFT−NEGF calculations confirm the modest current variation observed experimentally. DFT calculations show that the HOMO is largely located on the thiol group in these molecules, and this is the closest orbital to the Fermi energy of the electrodes. Therefore, the transport is hole-like. To understand the weak effect of the tail group on the conductance, we have constructed a tight-binding toy model with site energies and tunneling parameters based on a series of DFT arguments and existing literature. Our model reproduces the structure of the highest occupied orbitals (HOMO, HOMO-1, HOMO-2, and HOMO-3). Our analysis suggests a few reasons for the surprisingly small differences among the currents in these molecules with saturated and conjugated tails: (1) The location and the energy of the frontier orbitals which are responsible for the transport are similar across the entire series. For instance, the HOMO in all molecules is localized on the thiol linker. (2) The transmission is therefore mainly determined by the tunneling through the rest of the molecule, which is influenced by the tail group. In the tail groups, the differences between the values of the site energies (ε) and tunneling parameters (t) in the conjugated and saturated groups largely compensate each other: Conjugated groups have smaller coupling (than saturated ones) but their ε is much closer to the Fermi energy than is that for saturated groups. The combination of both still leads to better conductivity of the conjugated groups. However, the coupling of the tail group to the alkane chain (t_R') is much weaker for conjugated groups than for saturated ones. So the combination of t_R and t_R' compensates for the large difference between ε's in conjugated and saturated groups. (3) The conductance is also influenced by the broadening of the molecular levels connected to the left and right electrodes ($\Gamma_{L,R}$). In all these molecules Γ_L is the same and Γ_R is determined by the connection to the oxide layer. For the two molecules C_{12} and C_{18} (used as calibration standards) in which the length of the alkane tail group is extended, the coupling to the electrode decays exponentially, and therefore a significant change in the $I-V$ characteristic can be observed. We found that the decay constant is $\beta = 1.1$ per methylene group in alkanethiols which is in agreement with the experimental results ($\beta = 0.9-1.0$). We therefore expect the similarity of the current for saturated and conjugated tail groups to depend sensitively on the tail group length—longer tail groups would lead to saturated tail groups yielding lower current densities.

METHODS

NEGF−DFT Calculations. *(I). Gas Phase-NEGF.* In this method, DFT calculations for molecules in the gas phase (thiol-ended, without electrodes) are performed and then the contribution of the molecule to transport is calculated by computing $|G_{1N}{}^2|$ between the p_z orbitals (perpendicular to the plane through S, C, and H) of the S(1) and the R groups (N) where G denotes the Green's function and S is the sulfur atom of the thiol linker.[36] G_{1N} can be understood as the quantity which measures the tunneling amplitude from site 1 to site N. Once the Green's functions are known, the transmission can be obtained using the Landauer-type equation. Here we include self-energies within wide-band limit approximation.[37]

The coupling of the tail groups to the Ga_2O_3 oxide layer (on the EGaIn electrode) is an unknown parameter which is not included in the gas-phase calculations. This method does not yield the correct location of the transmission peaks (of the occupied orbitals) since the molecules are considered in gas phase—shifts induced by interface dipoles and image charges are therefore not taken into account. To obtain better insight into these shifts, we have used another method.

(II). Extended Molecule-NEGF. In this method, an *extended molecule* is used. The extended molecule is made by connecting the molecule to $3 \times 3 \times 3$ metal clusters from right and left. Then we connect this extended molecule to two electrodes which are $3 \times 3 \times 9$ clusters. For silver, we need to incorporate 19 electrons per silver atom for the largest frozen core, as opposed to 11 electrons per gold atom. In view of the similarity between the two contact types,[38] and since that we are looking for trends which are expected to be the same for silver and gold, we have chosen to perform our calculations using gold contacts. Experimentally, with a metal alloy and a conductive oxide

layer on one side of the molecule, the screening cannot be expected to let surface effects decay within the width of the contacts. We present the results for a molecule between two gold contacts as another reference calculation, with the awareness that the actual system (Ag on one side and oxide/metal on the other side) is somewhere in between that of the gas phase and the extended molecule with gold contacts.

To calculate the self-energies for each $3 \times 3 \times 9$ cluster, we divide the cluster into three layers in which each layer consists of three sublayers, as shown in Figure 3. Then we calculate the transport properties of the system. This method relies on the strong screening in the contact regions, which renders the results relatively insensitive to their size.

The code used here is an in-house developed add-on to the Amsterdam Density Functional (ADF) code[39] (using an LDA exchange correlation functional and a double-ζ polarized basis set).[36,39] The Fermi energy of the gold electrode in our calculations is -5.3 eV, which is taken as the midpoint between the HOMO and the LUMO of the $3 \times 3 \times 9$ Au cluster.

DFT Molecular Orbitals. DFT calculations for molecules 1−13 using the quantum chemistry codes ADF[39] and Q-chem[40] were performed with a TZP (triple zeta polarization) basis set, and a GGA exchange-correlation functional (PBE) in ADF, and 6-31G** basis set and PBE0 exchange correlation functional in Q-chem. Both codes give similar results. The ones shown in the paper and in the Supporting Information were obtained using ADF.

Conflict of Interest: The authors declare no competing financial interest.

Acknowledgment. F.M. gratefully acknowledges the hospitality of the M.A.R. group in Northwestern University and useful discussions with J. S. Seldenthuis and B. Movaghar. We thank H. J. Yoon for sharing the data of the measured current with us and F. C. Grozema (Delft) for valuable comments. Financial support was obtained from the EU FP7 program under the grant agreements SINGLE and ELFOS. Collaborative aspects of the research involving M.A.R. and G.M.W. were supported by the nonequilibrium energy research center (NERC), an Energy Frontier Research Center funded by the U.S. Department of Energy Office of Science, Office of Basic Energy Sciences under Award II DE−SC0000989. M.A.R thanks the Chem. Division of the NSF (CHE1058896) for support.

Supporting Information Available: Determination of the tight binding parameters; validation of the TBTM parameters; current obtained using the extended molecule This material is available free of charge *via* the Internet at http://pubs.acs.org.

REFERENCES AND NOTES

1. Yoon, H. J.; Shapiro, N. D.; Park, K. M.; Thuo, M. M.; Soh, S.; Whitesides, G. M. The Rate of Charge Tunneling through Self-Assembled Monolayers Is Insensitive to Many Functional Group Substitutions. *Angew. Chem., Int. Ed.* **2012**, *51*, 4658–4661.
2. Nitzan, A.; Ratner, M. A. Electron Transport in Molecular Wire Junctions. *Science* **2003**, *300*, 1384.
3. Paulsson, M.; Zahid, F.; Datta, S. Resistance of a Molecule. In *Handbook of Nanotechnology*; Goddard, W. A., III, Brenner, D. W., Lyshevski, S. E., Iafrate, G. J., Eds.; CRC Press: Boca Raton, FL, 2003.
4. Datta, S. *Quantum Transport: Atom to Transistor*; Cambridge University Press: Cambridge, UK, 2005.
5. Cuevas, J. C.; Scheer, E. *Molecular Electronics, an Introduction to Theory and Experiment*; World Scientific: Singapore, 2010.
6. Mujica, V.; Ratner, M. A. Current−Voltage Characteristics of Tunneling Molecular Junctions for off-Resonance Injection. *Chem. Phys.* **2001**, *264*, 365–370.
7. Galperin, M.; Ratner, M. A.; Nitzan, A.; Troisi, A. Nuclear Coupling and Polarization in Molecular Transport Junctions: Beyond Tunneling to Function. *Science* **2008**, *319*, 1056–1060.
8. Rampi, M. A.; Whitesides, G. M. A Versatile Experimental Approach for Understanding Electron Transport through Organic Materials. *Chem. Phys.* **2002**, *281*, 373–391.
9. Heersche, H. B.; Lientschnig, G.; O'Neill, K.; van der Zant, H. S. J.; Zandbergen, H. W. *In Situ* Imaging of Electromigration-Induced Nanogap Formation by Transmission Electron Microscopy. *Appl. Phys. Lett.* **2007**, *91*, 072107.
10. Park, H.; Lim, A. K. L.; Alivisatos, A. P.; Park, J.; McEuen, P. L. Fabrication of Metallic Electrodes with Nanometer Separation by Electromigration. *Appl. Phys. Lett.* **1999**, *75*, 301–303.
11. Fracasso, D.; Valkenier, H.; Hummelen, J. C.; Solomon, G. C.; Chiechi, R. C. Evidence for Quantum Interference in SAMs of Arylethynylene Thiolates in Tunneling Junctions with Eutectic Galn (EGaln) Top-Contacts. *J. Am. Chem. Soc.* **2011**, *133*, 9556–9563.
12. Arroyo, C.; Frisenda, R.; Moth-Poulsen, K.; Seldenthuis, J.; Bjornholm, T.; van der Zant, H. Quantum Interference Effects at Room Temperature in OPV-Based Single-Molecule Junctions. *Nanoscale Res. Lett.* **2013**, *8*, 234.
13. George, C.; Yoshida, H.; Goddard, W. A.; Jang, S. S.; Kim, Y.-H. Charge Transport through Polyene Self-Assembled Monolayers from Multiscale Computer Simulations. *J. Phys. Chem. B* **2008**, *112*, 14888–14897.
14. Dickey, M. D.; Chiechi, R. C.; Larsen, R. J.; Weiss, E. A.; Weitz, D. A.; Whitesides, G. M. Eutectic Gallium−Indium (EGaln): A Liquid Metal Alloy for the Formation of Stable Structures in Microchannels at Room Temperature. *Adv. Funct. Mater.* **2008**, *18*, 1097–1104.
15. Lee, T.; Wang, W.; Klemic, J. F.; Zhang, J. J.; Su, J.; Reed, M. A. Comparison of Electronic Transport Characterization Methods for Alkanethiol Self-Assembled Monolayers. *J. Phys. Chem. B* **2004**, *108*, 8742–8750.
16. Li, C.; Pobelov, I.; Wandlowski, T.; Bagrets, A.; Arnold, A.; Evers, F. Charge Transport in Single Au−Alkanedithiol−Au Junctions: Coordination Geometries and Conformational Degrees of Freedom. *J. Am. Chem. Soc.* **2008**, *130*, 318–326.
17. Xu, B.; Tao, N. J. Measurement of Single-Molecule Resistance by Repeated Formation of Molecular Junctions. *Science* **2003**, *301*, 1221–1223.
18. Slowinski, K.; Chamberlain, R. V.; Miller, C. J.; Majda, M. Through-Bond and Chain-to-Chain Coupling. Two Pathways in Electron Tunneling through Liquid Alkanethiol Monolayers on Mercury Electrodes. *J. Am. Chem. Soc.* **1997**, *119*, 11910–11919.
19. Smalley, J. F.; Feldberg, S. W.; Chidsey, C. E. D.; Linford, M. R.; Newton, M. D.; Liu, Y.-P. The Kinetics of Electron Transfer Through Ferrocene-Terminated Alkanethiol Monolayers on Gold. *J. Phys. Chem.* **1995**, *99*, 13141–13149.
20. Wold, D. J.; Frisbie, C. D. Formation of Metal−Molecule−Metal Tunnel Junctions: Microcontacts to Alkanethiol Monolayers with a Conducting AFM Tip. *J. Am. Chem. Soc.* **2000**, *122*, 2970–2971.
21. Bumm, L. A.; Arnold, J. J.; Dunbar, T. D.; Allara, D. L.; Weiss, P. S. Electron Transfer through Organic Molecules. *J. Phys. Chem. B* **1999**, *103*, 8122–8127.
22. Kaun, C.-C.; Guo, H. Resistance of Alkanethiol Molecular Wires. *Nano Lett.* **2003**, *3*, 1521–1525.
23. Akkerman, H. B.; de Boer, B. Electrical Conduction through Single Molecules and Self-Assembled Monolayers. *J. Phys: Condens. Matter* **2008**, *20*, 013001.
24. Fagas, G.; Delaney, P.; Greer, J. C. Independent Particle Descriptions of Tunneling Using the Many-Body Quantum Transport Approach. *Phys. Rev. B* **2006**, *73*, 241314.
25. Xue, Y.; Datta, S.; Ratner, M. A. First-Principles Based Matrix Green's Function Approach to Molecular Electronic Devices: General Formalism. *Chem. Phys.* **2002**, *281*, 151–170.
26. Brandbyge, M.; Mozos, J.-L.; Ordejón, P.; Taylor, J.; Stokbro, K. Density-Functional Method for Nonequilibrium Electron Transport. *Phys. Rev. B* **2002**, *65*, 165401.
27. Hoffmann, R. An Extended Huckel Theory. I. Hydrocarbons. *J. Chem. Phys.* **1963**, *39*, 1397–1412.
28. Pariser, R.; Parr, R. G. A Semi-empirical Theory of the Electronic Spectra and Electronic Structure of Complex Unsaturated Molecules. I. *J. Chem. Phys.* **1953**, *21*, 466–471.
29. Pople, J.; Beveridge, D. *Approximate Molecular Orbital Theory*; McGraw-Hill: New York, 1970.

30. Dewar, M. J. S.; Thiel, W. Ground States of Molecules. 38. The MNDO Method. Approximations and Parameters. *J. Am. Chem. Soc.* **1977**, *99*, 4899–4907.
31. Benkö, G.; Flamm, C.; Stadler, P. F. A Graph-Based Toy Model of Chemistry. *J. Chem. Inf. Comput. Sci.* **2003**, *43*, 1085–1093, PMID: 12870897.
32. Xu, C. H.; Wang, C. Z.; Chan, C. T.; Ho, K. M. A Transferable Tight-Binding Potential for Carbon. *J. Phys.: Condens. Matter* **1992**, *4*, 6047.
33. Wang, Y.; Mak, C. Transferable Tight-Bonding Potential for Hydrocarbons. *Chem. Phys. Lett.* **1995**, *235*, 37–46.
34. Murrell, J. N. *The Theory of the Electronic Spectra of Organic Molecules*; John Wiley and Sons Inc: New York; Methuen and Co. LTD: London, 1963.
35. Salem, L. *Molecular Orbital Theory of Conjugated Systems*; W.A. Benjamin, Inc.: New York, 1966.
36. Verzijl, C. J. O.; Seldenthuis, J. S.; Thijssen, J. M. Applicability of the Wide-Band Limit in DFT-Based Molecular Transport Calculations. *J. Chem. Phys.* **2013**, *138*, 094102.
37. Jauho, A.-P.; Wingreen, N. S.; Meir, Y. Time-Dependent Transport in Interacting and Noninteracting Resonant-Tunneling Systems. *Phys. Rev. B* **1994**, *50*, 5528–5544.
38. Lawson, J. W.; Bauschlicher, C. W. Transport in Molecular Junctions with Different Metallic Contacts. *Phys. Rev. B* **2006**, *74*, 125401.
39. *ADF2010*; Scientific Computing & Modeling: Amsterdam, The Netherlands, 2010; http://www.scm.com.
40. Shao, Y.; Molnar, L. F.; Jung, Y.; Kussmann, J.; Ochsenfeld, C.; Brown, S. T.; Gilbert, A. T.; Slipchenko, L. V.; Levchenko, S. V.; O'Neill, D. P.; *et al.* Advances in Methods and Algorithms in a Modern Quantum Chemistry Program Package. *Phys. Chem. Chem. Phys.* **2006**, *8*, 3172–3191.